

REPORT DOCUMENTATION PAGE				Form Approved OMB No. 0704-0188	
<p>Public reporting burden for this collection of information is estimated to average 1 hour per response, including the time for reviewing instructions, searching existing data sources, gathering and maintaining the data needed, and completing and reviewing this collection of information. Send comments regarding this burden estimate or any other aspect of this collection of information, including suggestions for reducing this burden to Department of Defense, Washington Headquarters Services, Directorate for Information Operations and Reports (0704-0188), 1215 Jefferson Davis Highway, Suite 1204, Arlington, VA 22202-4302. Respondents should be aware that notwithstanding any other provision of law, no person shall be subject to any penalty for failing to comply with a collection of information if it does not display a currently valid OMB control number. <b>PLEASE DO NOT RETURN YOUR FORM TO THE ABOVE ADDRESS.</b></p>					
1. REPORT DATE (DD-MM-YYYY) June 2012		2. REPORT TYPE Journal Article		3. DATES COVERED (From - To) Jan – Jun 2012	
4. TITLE AND SUBTITLE Performance and Thrust-to-Weight Optimization of the Dual-Expander Aerospike Nozzle Upper Stage Rocket Engine				5a. CONTRACT NUMBER In-House	
				5b. GRANT NUMBER	
				5c. PROGRAM ELEMENT NUMBER	
6. AUTHOR(S) Hall, Joshua N.; Hartsfield, Carl R.; Simmons, Joseph R.; Branam, Richard D.				5d. PROJECT NUMBER	
				5e. TASK NUMBER	
				5f. WORK UNIT NUMBER 50260651/Q0BD	
7. PERFORMING ORGANIZATION NAME(S) AND ADDRESS(ES) Air Force Research Laboratory (AFMC) AFRL/RZSE 4 Draco Drive Edwards AFB, CA 93524-7160				8. PERFORMING ORGANIZATION REPORT NO.	
9. SPONSORING / MONITORING AGENCY NAME(S) AND ADDRESS(ES) Air Force Research Laboratory (AFMC) AFRL/RZS 5 Pollux Drive Edwards AFB, CA 93524-7048				10. SPONSOR/MONITOR'S ACRONYM(S)	
				11. SPONSOR/MONITOR'S REPORT NUMBER(S) AFRL-RZ-ED-JA-2012-168	
12. DISTRIBUTION / AVAILABILITY STATEMENT Approved for public release; distribution unlimited					
13. SUPPLEMENTARY NOTES PA Case Number: 12413, Clearance Date: 7 Jun 2012					
14. ABSTRACT  <p>The Air Force Institute of Technology (AFIT) is designing a cryogenic Dual-Expander Aerospike Nozzle (DEAN) upper stage rocket engine. The design goals for the engine are reusability, 50,000 pounds-force (222 kilonewtons) vacuum thrust, 464 seconds of vacuum specific impulse and a thrust-to-weight ratio of 106.5. Utilizing past AFIT work as a foundation, an enhanced system-level design model was created that conservatively estimates engine performance and weight. The assumptions and resulting engine designs of this study highlight important design choices (i.e. material selection). This study discusses an engine design meeting the engine thrust-to-weight ratio and reusability design goals but falling short of the vacuum specific impulse design goal. The study shows the DEAN design is competitive to current operational upper stage engines. Potential future assumptions and design choices are identified and warrant further study.</p>					
15. SUBJECT TERMS Aerospike Nozzle, rocket engine					
16. SECURITY CLASSIFICATION OF:			17. LIMITATION OF ABSTRACT	18. NUMBER OF PAGES	19a. NAME OF RESPONSIBLE PERSON
a. REPORT	b. ABSTRACT	c. THIS PAGE			Gregory A. Ruderman
Unclassified	Unclassified	Unclassified	SAR	31	19b. TELEPHONE NO (include area code) 661-275-5332

# **Performance & Thrust-to-Weight Optimization of the Dual-Expander Aerospike Nozzle Upper Stage Rocket Engine**

Joshua N. Hall<sup>1</sup>

*Air Force Research Laboratory, Edwards AFB, CA, 93524*

Carl R. Hartsfield<sup>2</sup> and Joseph R. Simmons<sup>3</sup>

*Air Force Institute of Technology, Dayton, OH, 45433*

Richard D. Branam<sup>4</sup>

*Air University, Montgomery, AL, 36112*

**The Air Force Institute of Technology (AFIT) is designing a cryogenic Dual-Expander Aerospike Nozzle (DEAN) upper stage rocket engine. The design goals for the engine are reusability, 50,000 pounds-force (222 kilonewtons) vacuum thrust, 464 seconds of vacuum specific impulse and a thrust-to-weight ratio of 106.5. Utilizing past AFIT work as a foundation, an enhanced system-level design model was created that conservatively estimates engine performance and weight. The assumptions and resulting engine designs of this study highlight important design choices (i.e. material selection). This study discusses an engine design meeting the engine thrust-to-weight ratio and reusability design goals but falling short of the vacuum specific impulse design goal. The study shows the DEAN design is competitive to current operational upper stage engines. Potential future assumptions and design choices are identified and warrant further study.**

---

<sup>1</sup> Program Manager, Third Generation Reusable Boost, Air Force Research Laboratory, Edwards AFB, CA 93524, Member.

<sup>2</sup> Assistant Professor, Graduate School of Engineering and Management, Department of Aeronautics and Astronautics, 2950 Hobson Way, WPAFB, OH 45433, Member.

<sup>3</sup> PhD Student, Graduate School of Engineering and Management, Department of Aeronautics and Astronautics, 2950 Hobson Way, WPAFB, OH 45433, Student Member.

<sup>4</sup> Assistant Professor, Air War College, Air University, 325 Chennault Circle, Maxwell AFB, AL 36112, AIAA Associate Fellow.

## Nomenclature

$A^*$	=	throat area (in <sup>2</sup> )
$F$	=	total thrust (lb <sub>f</sub> )
$F_{nondesign}$	=	thrust component due to nozzle operation at altitudes other than the design altitude (lb <sub>f</sub> )
$F_{cowl}$	=	thrust component acting on the chamber exit lip (lb <sub>f</sub> )
$\dot{m}$	=	total propellant flow rate (lb <sub>m</sub> /s)
$O/F$	=	oxidizer-to-fuel ratio
$p^*$	=	throat pressure (psia)
$p_{amb}$	=	ambient pressure (psia)
$p dA$	=	pressure acting on the nozzle at differential cross-sectional areas
$\theta$	=	angle of flow to the centerline of the spike (deg)
$T/W$	=	thrust-to-weight ratio
$v^*$	=	throat velocity (ft/s)

## I. Introduction

CURRENT operational upper stage rocket engine technology has proven successful to meet orbit transfer needs. However, the United States Air Force recognizes major technological improvements are required to meet future demands, especially in the area of specific impulse and engine thrust-to-weight ratio ( $T/W$ ) [1]. The Air Force is making strides forward with the goal of first maturing upper stage engine technology and secondly incorporating the mature technology in future operational designs [2, 3]. The Air Force Institute of Technology (AFIT) is joining the cause of upper stage engine improvements with a novel engine concept: a reusable dual-expander aerospike nozzle rocket engine, referred to as the DEAN.

The DEAN utilizes liquid hydrogen and liquid oxygen as propellants, is powered by two separate expander cycles to pump the propellants and utilizes an aerospike nozzle for improved performance compared to a conventional bell nozzle. The design goals for the engine are reusability, 50,000 lb<sub>f</sub> (222 kN) vacuum thrust, 464 seconds of vacuum specific impulse and a thrust-to-weight ratio of 106.5. Designing the engine to be reusable allows the engine to be robust against testing and survive multiple flight restarts.

Both Martin and Simmons performed foundational DEAN design work at AFIT. Martin first demonstrated the feasibility of the DEAN concept at a single design point [4]. Simmons followed with the creation of a system level model enabling parametric trade studies of the solution space and improvements to the DEAN design [5].

Hall, building upon previous AFIT work, enhanced the system level DEAN model to estimate engine performance, weight and geometry reliably [6]. Parametric trade and optimization studies of the solution space found a new DEAN design point that met most of the design goals without violating physical and reusability constraints; unfortunately, the vacuum specific impulse goal was not met by 33.4 seconds or 7.3%. Although unable to meet all the design goals, the best DEAN concept proves to be competitive to current operational and under development upper stage engines.

## **II. DEAN Concept**

The DEAN differs from other cryogenic upper stage engines in two ways. First, the engine utilizes separate expander cycles for the oxidizer and fuel. Second, the engine utilizes an aerospike nozzle.

In a traditional expander cycle, the fuel alone regeneratively cools the combustion chamber and nozzle. The heat transferred to the fuel from cooling provides enough power to the turbine to power both the fuel and oxidizer pumps prior to the injection of the fuel into the combustion chamber. The DEAN employs an oxidizer expander cycle to drive the oxidizer pump and similarly a fuel expander cycle to drive the fuel pump [7]. The fuel and oxidizer remain physically separated until injection into the combustion chamber, eliminating the need for an interpropellant seal; failure of this seal is the critical catastrophic failure mode in traditional expander cycle engines [4].

Figure 1 is a sketch of the two independent expander cycles with fuel and oxidizer flow represented on the left and right side of the figure, respectively. The propellant first travels from the propellant tank through the pump. The pump increases the propellant pressure and then delivers the propellant to the cooling jacket where the propellant gains energy from regenerative cooling of the combustion chamber (oxygen) or aerospike (hydrogen). The cooling jacket also keeps the combustion chamber and aerospike temperatures below structural thermal limits. The additional energy in the propellant from regenerative cooling drives the turbine/expander cycle. From the turbine, the propellant travels to the injectors and into the combustion chamber for combustion. Lastly, the combusted products (exhaust) expand against the aerospike nozzle to produce the desired performance. In the oxidizer expander cycle, a small percentage of the warm oxygen bypasses the turbine to the injectors to control and balance the engine cycle.

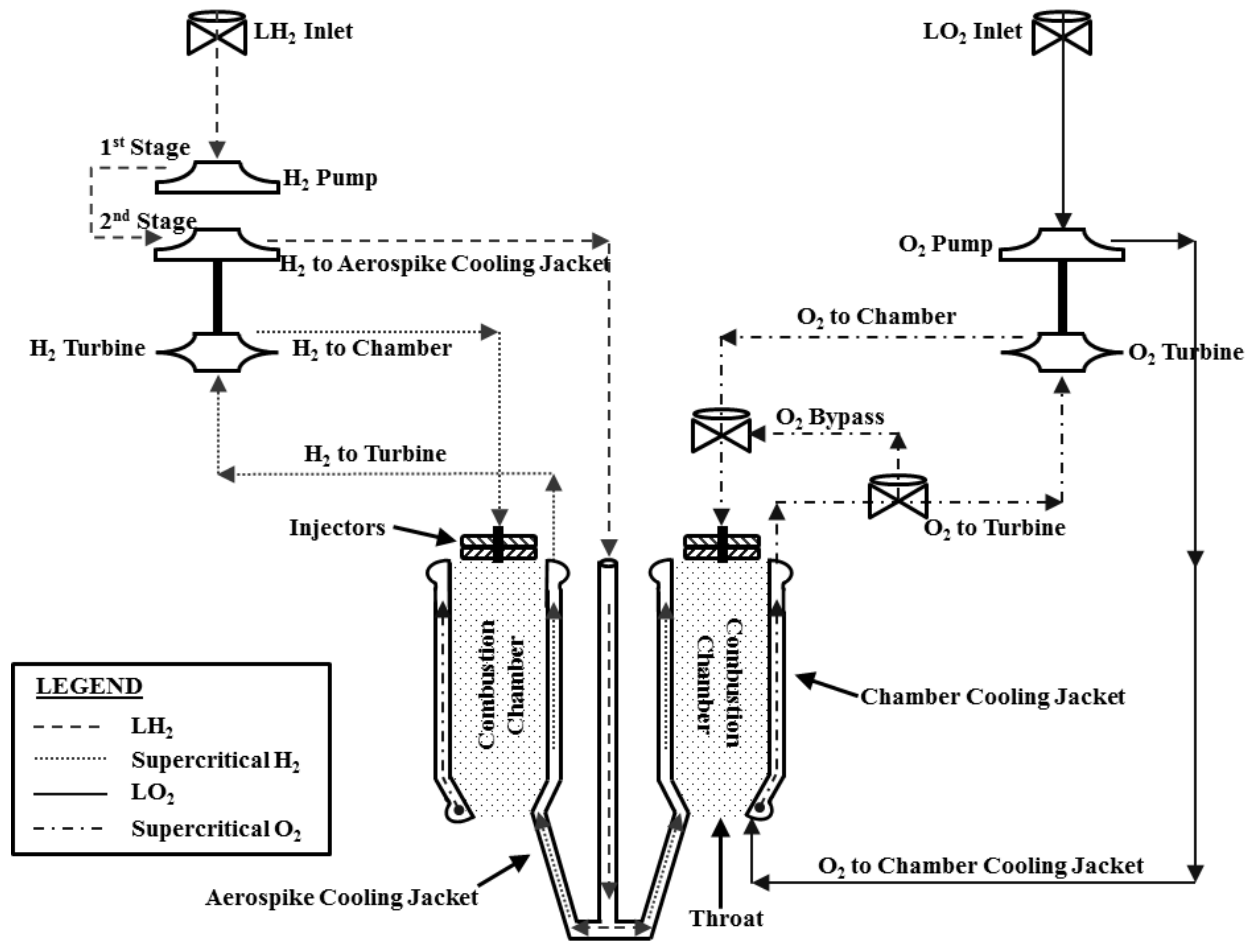


Figure 1 Schematic of DEAN engine

The DEAN nozzle contains an annular aerospike nozzle, also known as a radial in-flow plug nozzle. An annular aerospike nozzle consists of a longitudinally elongated annulus forming a cylinder (the combustion chamber) with a specially designed spike in the center of it. Although not a benefit for an upper stage engine operating in vacuum, the aerospike nozzle can operate near optimally at all altitudes below or at its design altitude. More specifically, the aerospike can compensate for changes in altitude and ambient conditions, meaning the aerospike nozzle will not suffer from the same overexpansion losses a bell nozzle suffers [8]. Above its design altitude, the aerospike nozzle behaves more like a conventional bell nozzle losing its altitude compensation capabilities. For orbit transfer missions, rocket engines require a high expansion ratio increasing the length and mass of a traditional bell nozzle. The benefit of using an aerospike nozzle for upper stage applications is the engine will be shorter and lighter than a bell nozzle with equivalent performance, especially if the aerospike nozzle is truncated. Previous work utilized the

full aerospike nozzle length to explore highest achievable specific impulse performance; however, Martin did show performance degradation is limited with a truncated spike [4].

Utilizing an aerospike nozzle enables the use of the dual-expander cycle. Aerospike nozzle geometry, with two distinct walls requiring cooling, can serve to separate the fuel and oxidizer until injection into the combustion chamber. Physical separation of the propellants during regenerative cooling lends itself to the dual-expander cycle. The two distinct walls also provide a greater surface area for heat transfer at the throat compared to a bell nozzle. This increase in heat transfer surface area means more power to the turbine, increased chamber pressure, and increased performance compared to regenerative cooling in a bell nozzle. Aerospike geometry with a larger throat surface area means each propellant can gain enough energy to power its own expander cycle.

The DEAN concept consists of twelve main engine components: combustion chamber and aerospike cooling jackets, combustion chamber and aerospike structural jackets, aerospike nozzle tip, two turbopump assemblies (pump, turbine and shaft combination), plumbing for each propellant, injectors, oxidizer dome and hardware. The term aerospike is represented by the entire surface of the inner combustion chamber wall plus the aerospike nozzle. The cooling jackets serve to physically separate the hot combusted products from the coolant while maximizing heat transfer to the coolant to power the turbopumps. The structural jackets serve to restrain the cooling channel and combustion chamber pressures. The aerospike nozzle tip is the uncooled portion of the aerospike nozzle. Two turbopumps exist; one for the fuel and the other for the oxidizer to power the individual expander cycles. Plumbing exists for both the fuel and oxidizer and serves as a physical boundary to move propellant from one engine component to another. Linked to the plumbing components are manifolds located at each end of the propellant cooling jackets. One manifold serves to distribute the propellant into the cooling channels and the other serves to collect the propellant from the cooling channels directing the propellant into a single pipe towards the turbine. The oxidizer dome serves as a manifold to transfer the propellant into the injectors and into the combustion chamber. Hardware accounts for rivets, nuts, bolts, wiring, etc. Figure 2 is an axial view of the DEAN concept showing the aerospike and combustion chamber structural and cooling jackets. The concept assumes fifty percent of the full-length aerospike nozzle is cooled.

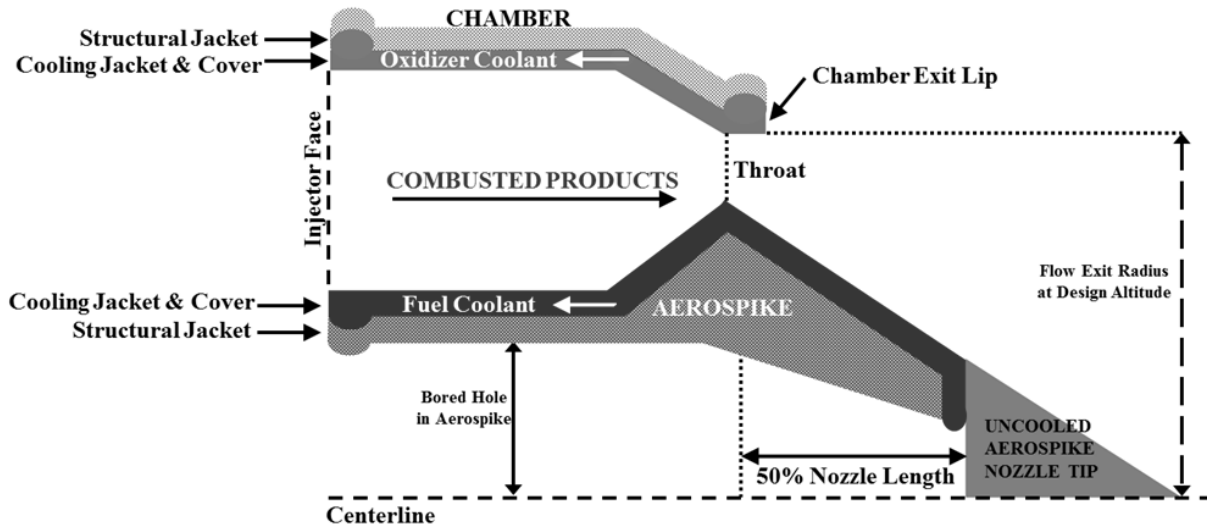


**Figure 2 Axial geometry for the DEAN chamber and aerospike**

### III. Previous DEAN Work

Martin's efforts involved building the first DEAN computational model, an engine power balance tool, using the Numerical Propulsion System Simulation (NPSS<sup>TM</sup>) software tool [4]. NPSS, designed by the National Aeronautics and Space Administration (NASA) and the aerospace propulsion industry, is a computer simulation tool for modeling aircraft and rocket propulsion systems [9]. The DEAN model designed by Martin includes NPSS elements linked together to accurately represent DEAN engine components such as the combustion chamber, aerospike nozzle, tanks, plumbing, cooling jackets, and turbopumps. Using his DEAN NPSS model, Martin performed an engine power balance at a single design point. This design point not only met, but also exceeded the design performance goals proving the feasibility of the engine. Table 1 tabulates the performance parameters of the DEAN at the design point found by Martin [4].

**Table 1 Past DEAN work design performance comparison**

Performance Parameters	Design Goals	Martin's Design Point [4]	Simmons' Design Point [5]
Vacuum Thrust	50,000 lbf (222 kN)	57,000 lbf (254 kN)	50,900 lbf (226 kN)
Vacuum Specific Impulse	464 sec	472 sec	489 sec

In parameterizing Martin's NPSS model, Simmons simplified the geometry of the aerospike nozzle and cooling volumes to linear approximations from higher order calculations; for example, Martin [4] calculated the aerospike nozzle radii using the method of characteristics in a separate effort [5]. Furthermore, with fixed DEAN performance goals, Simmons altered the design variables to support optimization studies focusing on minimizing engine weight

and maximizing engine  $T/W$ . Since geometry and material selection drive chamber and aerospike weight and the propellant mass flows drive turbopump weight, the NPSS model design variables were changed to chamber and aerospike geometries and the propellant mass flows to the turbopumps. These modifications to Martin's NPSS model enabled Simmons to create a system level model.

Simmons built the system level model of the DEAN using the ModelCenter<sup>TM</sup> software by Phoenix Integration. ModelCenter is a diverse modeling tool allowing designers to quickly and efficiently examine design trade spaces and perform optimization studies within user-specified design constraints. The DEAN system level model contained the parametric NPSS DEAN model along with other required modeling elements, such as capability to calculate fluid Mach numbers through the engine [5].

Simmons performed parametric trade studies with the model over varying chamber lengths, oxidizer-to-fuel ratios ( $O/F$ ), and total engine mass flow rates to determine design trade space boundaries. The results of the trade studies were significant in finding a new starting point for future optimization studies (i.e. a potential optimal  $O/F$  value) and discovering if the fluid Mach numbers through the engine plumbing and cooling jackets were within reasonable subsonic limits. Through the trade studies, Simmons found a design point meeting the performance design goals while reducing the system level weight of the turbopumps/engine and reducing the overall engine length by 25% compared to Martin's original design point. Table 1 tabulates the performance parameters for Simmons' new design point along with the DEAN's performance goals [5].

#### **IV. Enhanced System Level DEAN Model**

Hall further enhanced the system level model created by Simmons in ModelCenter and performed parametric trade and optimization studies to find a new DEAN design point providing maximum  $T/W$ , while meeting the performance design goals and not violating physical and reusability constraints [6]. The physical constraints involved maximum wall temperatures less than the material melting point, maximum wall stress less than the material ultimate strength, and a maximum fluid Mach number through the engine less than 0.6 and 0.9 for oxygen and hydrogen [4], respectively. The reusability constraints included maximum wall stress less than the material yield strength and maximum wall temperatures less than 60% the material melting point. Common metals, alloys, and ceramics were evaluated in the model to improve near-term manufacturability of the DEAN engine.



## A. Model Overview

A brief description of the model will be presented. A more detailed description of the model, including all assumptions, logic, equations, and verification and validation cases, is provided by Hall [6]. The enhanced DEAN model provides improved accuracy in estimating system level performance and weight by removing linear approximations, replacing them with nonlinear calculations and by incorporating added physics into the model. Furthermore, physical and reusability constraints were added to the model.

Similar to Simmons' model, the enhanced model uses ModelCenter and NPSS along with two additional software tools: Two-Dimensional Kinetics '04 (TDK'04<sup>TM</sup>) by Software and Engineering Associates, Inc. (SEA) and Chemical Equilibrium with Applications (CEA<sup>TM</sup>) by NASA. ModelCenter provides a user-friendly architecture to create a system-level model with the additional capability to perform model parametric trade and optimization studies. NPSS serves to perform an overall engine power balance accounting for each expander cycle. TDK'04 performs axisymmetric method of characteristics (MOC) calculations for aerospike nozzle geometry and CEA is required to perform chemistry calculations as an input into TDK'04. To use TDK'04 properly, the length of the aerospike nozzle was calculated using the Angelino approximation method [10].

The enhanced model contains four main assemblies each with multiple subassemblies, subcomponents, and/or convergence loops:

- 1) The first main assembly is "DesignVariables" containing all the system level variables required to execute the model. The main variables are the oxidizer-to-fuel ratio ( $O/F$ ), the engine mass flow rate ( $\dot{m}$ ), combustion chamber length, aerospike and chamber radius at the injector face, material selection for the aerospike and chamber cooling jackets, aerospike and chamber structural jackets, aerospike nozzle tip, and oxygen and hydrogen plumbing. Focusing on engine  $T/W$  optimization, engine mass flow rate was selected as a model input causing throat area and chamber pressure to be model outputs.

- 2) The second assembly is "Linear\_DEAN\_Model"; the assembly executes the linear NPSS DEAN model to provide valid input estimates to the third assembly, "NonLinear\_DEAN\_Model". The linear NPSS model utilizes linear approximations developed by Simmons [5] for the aerospike nozzle and uses bell nozzle performance calculations.

- 3) The third assembly, "NonLinear\_DEAN\_Model", will execute TDK and the nonlinear NPSS model to calculate aerospike nozzle geometry and certify the fluid mechanics and thermo chemistry of the DEAN satisfy

governing laws. Both the linear and nonlinear NPSS models are similar in that they both balance the engine expander cycles and both assume linear approximations for the aerospike geometry internal to the combustion chamber; however, the two models differ in what aerospike nozzle geometry is used and how they calculate nozzle performance. Using an iterative approach, the nonlinear NPSS model utilizes the nonlinear aerospike nozzle geometry from TDK and calculates the momentum thrust of the engine. The output momentum thrust from the nonlinear NPSS model is used in combination with other ModelCenter elements in the “DEAN\_Post\_Processing” assembly (i.e. the nozzle pressure thrust calculated in TDK) to estimate total engine performance independently.

4) The last assembly is “Post-Processing”; the assembly post-processes the TDK and NPSS data, such as calculating the cooling jacket wall temperatures, designing the chamber and aerospike structural jackets, and calculating overall engine performance and weight. “Post\_Processing” also renders the geometry of the DEAN. Figure 3 shows the overall enhanced system level DEAN model with rendered geometry; note each arrow in the rendered geometry is 12 inches in length.

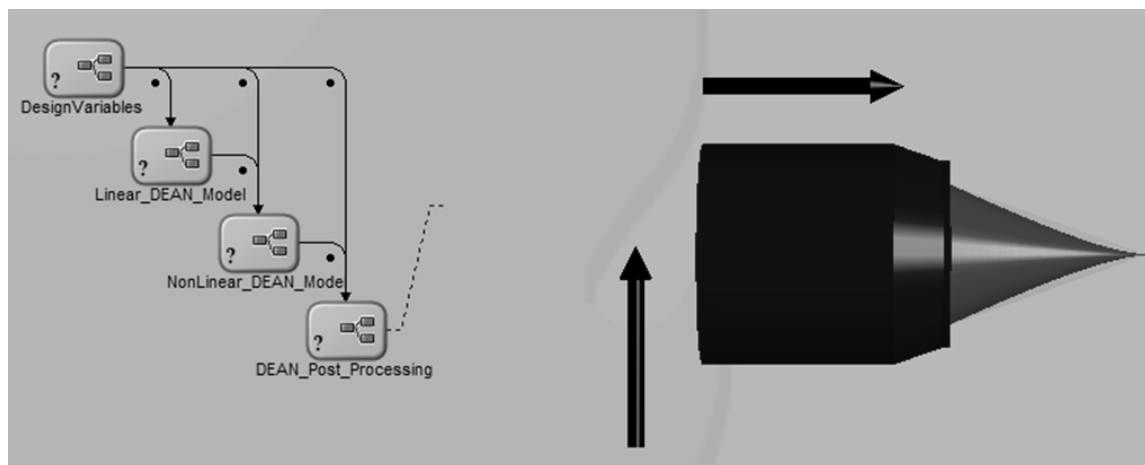


**Figure 3 Enhanced system level ModelCenter DEAN model**

Having both the linear and nonlinear NPSS models in the enhanced DEAN model proved necessary for successful model execution. Due to the nonlinear geometry of the cooling jacket along the first fifty percent of the aerospike nozzle extending from the throat, the nonlinear NPSS model required very accurate “guesses” to converge on a solution. The linear NPSS model converged much easier with user-input educated guesses and the solution provided very good input guesses for chamber pressure, throat area, pressure, enthalpy, and density profiles as inputs into the nonlinear NPSS model.

An attempt was made to parameterize the turbopump inputs into the NPSS model using processes by Humble *et al*, including turbopump efficiency maps [11]. Unfortunately, implementation resulted in the NPSS model

becoming very stiff especially with changes in turbopump shaft speed; although changes in pump and turbine efficiency values did work. The decision was made to keep the turbopump values constant, summarized in Table 2 (Martin [4]), for the remainder of the work effort. Future efforts need to incorporate dynamic turbopump models to improve fidelity and functionality of the optimization model.

**Table 2 Turbopump parameters from Martin [4]**

OXIDIZER	
Pump Efficiency	0.773
Pump Gear Ratio	1
Turbine Efficiency	0.949
Shaft Mechanical Speed (rpm)	32,000
FUEL	
Pump #1 Efficiency	0.8
Pump #1 Gear Ratio	1
Pump #2 Efficiency	0.83
Pump #2 Gear Ratio	1
Turbine Efficiency	0.9
Shaft Mechanical Speed (rpm)	110,000

Multiple studies were performed comparing the accuracy of linear calculations to nonlinear calculations in the model. The results showed the linear performance calculations provided results with 1% difference of the nonlinear performance calculations; for a system-level model/analysis, this difference is insignificant. However, there was a distinct difference in estimating the weight of the aerospike nozzle. The nonlinear calculations, using the method of characteristics nozzle geometry, provided a more accurate estimate for the actual weight of the component. The linear calculations result in higher component weight and may be preferred in system level weight estimation, adding conservatism to the estimated total engine weight and thrust-to-weight ratio. The more precise enhanced DEAN model with nonlinear calculations is utilized in this study.

## **B. Engine Performance Estimation**

Past DEAN work assumed an expansion ratio based on underexpanded flow (flow expands outward radially from chamber exit lip) due to operation in a vacuum and noting conventional bell nozzle upper stage engines physically require large expansion ratios to achieve desired performance. More research shows the nozzle expansion ratio is a function of outer chamber geometry and throat area defining the design altitude of the aerospike nozzle. The value of the expansion ratio is extremely important in the DEAN design since engine performance calculated in the linear NPSS model is strongly dependent on the expansion ratio. Furthermore, the method of

characteristics calculates aerospike nozzle geometry at the nozzle design altitude. At the nozzle design altitude, the exhaust flow at the chamber exit lip will follow a parallel path from the centerline to the exit plane [12].

The Angelino approximation method for an axisymmetric plug nozzle was employed to determine throat geometry for an aerospike engine designed to operate in near vacuum conditions (1 Pascal); the DEAN being an upper stage has a vacuum operational environment [10]. The results gave an unmanufacturable throat with a fluid flow passage between the chamber and aerospike at the throat of 1/1000 inch ( $2.54\text{e-}3$  cm). Furthermore, the approximation resulted in unrealistic chamber and aerospike throat radii and aerospike length, proving a near vacuum equivalent design altitude is not practical. Therefore, a more realistic nozzle design for an upper stage aerospike engine would be a lower design altitude (higher ambient pressure).

With a lower engine design altitude and operation in the vacuum of space, the aerospike nozzle exhaust flow will expand radially outward from the chamber exit lip and the nozzle overall will behave more like a conventional bell nozzle [8, 12]. How much the flow expands radially outward depends on the interaction of the flow with the ambient conditions; as a result, the flow exit area and engine expansion ratio are variable. The flow exit area will at least be equal to the chamber exit lip, or cowl, area (design altitude exit area) defining a minimum expansion ratio based on engine geometry for operation at or above the nozzle design altitude.

Using the same design variable inputs, Table 3 compares the performance for an assumed expansion ratio of 125 (used in previous work) and the performance parameters for Simmons' DEAN geometry operating at its design altitude using the linear NPSS model. The linear NPSS model results in an expansion ratio and engine performance using the chamber exit lip radius input and the calculated NPSS throat area. The calculated expansion ratio based on nozzle geometry is much less than the assumed expansion ratio showing current performance calculations are less than those previously determined.

**Table 3 Comparison of performance parameters due to expansion ratio**

	DEAN Model - Assumed Expansion Ratio [5]	Linear DEAN Model - Calculated Expansion Ratio [6]
Expansion Ratio	125	4.16
Vacuum Thrust	50,900 lb <sub>f</sub> (226 kN)	40,396 lb <sub>f</sub> (179.7 kN)
Vacuum Specific Impulse	489 s	388 s

For aerospike nozzles, the design altitude expansion ratio is a more accurate approach to engine performance estimation, as opposed to assuming an expansion ratio. Aerospike nozzle performance is improved by increasing the expansion ratio by geometrically increasing the chamber exit lip radius and/or decreasing the throat area.

Hall completed basic engine performance verification and validation of Simmons' DEAN system level model [5]. With the input expansion ratio, the system level model by Simmons calculated similar performance compared to the ideal rocket performance equations and CEA. All of Simmons' trade studies were re-accomplished and compared with the enhanced linear NPSS model. Simmons' and Hall's results were nearly identical with only small magnitude differences (consistent with a decreased expansion ratio), proving the change in expansion ratio does not influence validity of the enhanced DEAN model [6].

The linear DEAN NPSS model relies on bell nozzle design performance calculations. For the aerospike, the equation to calculate thrust is slightly different. According to Sutton and Biblarz, the thrust of an aerospike nozzle consists of three components [13]. First, there is the axial thrust component through the throat; momentum thrust. Second, the pressure distribution or integral of pressure acting on the length of the aerospike over the spike cross-sectional area; nozzle pressure thrust. Third, if the aerospike is truncated, the pressure acting over the base area; base pressure thrust. The sum of the three thrust components equals the total thrust value ( $F$ ) for the engine. The equation presented by Sutton and Biblarz does not account for the "negative effect of the slipstream of air around the engine (which causes a low-pressure region) and the friction on the aerospike" [13]. The third thrust component only applies if the full-length aerospike nozzle is truncated.

For a truncated nozzle, the subsonic recirculating flow acting along the truncated nozzle base (base flow) will interact with the primary exhaust flow. This interaction leads to the subsonic base flow forming an aerodynamic spike that mimics an ideal isentropic spike [8]. The main exhaust flow will continue to expand against the subsonic base flow. How much the exhaust flow expands along the aerodynamic spike may vary. Instead of performing a detailed computational analysis of the flow field during system level nozzle truncation studies, the enhanced DEAN model assumes the flow fully expands to the full-length aerospike exit pressure. With this assumption, the truncation thrust component is negligible.

Another thrust component exists, designated  $F_{nondesign}$ , when the nozzle operates at altitudes other than the design altitude.  $F_{nondesign}$  is a function of nozzle exit area and the difference between the ambient and nozzle exit pressures. In the enhanced DEAN model this thrust component is independent of nozzle truncation due to the full flow expansion assumption.

The estimated total system level thrust ( $F$ ) for the DEAN, regardless if the nozzle is truncated or full-length, is equivalent to equation 1:

$$F = [\dot{m}v^* \cos \theta + (p^* - p_{amb})A^*] + \int^A pdA + F_{nondesign} + F_{cowl} \quad (1)$$

where  $\dot{m}$  is the total propellant flow rate,  $v^*$  is the throat velocity,  $\theta$  is the angle of flow to the centerline of the spike,  $p^*$  is the throat pressure,  $p_{amb}$  is the ambient pressure,  $A^*$  is the throat area,  $pdA$  is the pressure acting on the nozzle at differential cross-sectional areas,  $F_{nondesign}$  is the thrust component due to nozzle operation at altitudes other than the design altitude, and  $F_{cowl}$  is the thrust acting on the chamber exit lip (calculated in TDK'04). The total thrust value takes into account aerospike nozzle viscous losses. Specific impulse is calculated as a function of total thrust and engine weight flow.

### C. Engine Weight and Thrust-to-Weight Ratio Estimation

Seven DEAN components utilize material properties for structural analyses and weight estimation. Material selection is required for the combustion chamber and aerospike structural and cooling jackets, the aerospike nozzle tip (also known as the uncooled portion of the aerospike nozzle), and the oxygen and hydrogen plumbing. The mass of the injectors and oxidizer dome are assumed part of the combustion chamber and aerospike masses and the mass of the manifolds at the start and end of the cooling jackets are assumed part of the cooling jacket mass.

Thirteen different materials were selected for the DEAN design based on their compatibility with the propellants. Table 4 summarizes the materials used in the DEAN model and summarizes what materials are useable for the individual engine components. Some materials are useable only if they are not exposed to the propellants (i.e. aluminum and titanium). In addition, different materials are useable for different engine components. The interaction of dissimilar metals is realistic; however, there are varieties of methods available to minimize galvanic corrosion. The DEAN model assumes galvanic corrosion is not an influential design factor.

The material properties utilized in the DEAN model include material density, material melting point, thermal conductivity, ultimate tensile strength, and yield strength. The properties, where appropriate, are coded as functions of temperature to improve accuracy to the structural analyses for the walls separating the coolant and combusted gases; these walls experience both hot chamber temperatures and cold coolant temperatures. Material properties, collected from [14-22], are a function of how the engine components are manufactured and of the purity of the material. Future work should further evaluate the material properties for more accurate heat transfer and mass estimation calculations.

**Table 4 Materials compatible with engine components**

Material	Propellant Compatibility / Selected Use on DEAN
Pure Copper (Annealed)	Compatible with O <sub>2</sub> and H <sub>2</sub> / Useable for chamber and aerospike cooling jacket, structural jacket, and O <sub>2</sub> and H <sub>2</sub> plumbing
Silicon Carbide (Highly-Pure)	
INCOLOY® 909 (Age Hardened)	
HAYNES® 188 alloy (Bright Annealed)	
Beryllium Copper (C17000 TH04)	
Oxygen-Free Copper (C10100 1180 Temper)	
Cobalt (Forged Electrolytic)	Compatible with O <sub>2</sub> / Useable for chamber cooling jacket, structural jacket, and O <sub>2</sub> plumbing
INCONEL® 718 (Annealed & Aged)	
INCONEL® 625 (Annealed)	
Aluminum 7075 T6	Not compatible with O <sub>2</sub> or H <sub>2</sub> / Useable for chamber and aerospike structural jacket as long as propellant contact does not occur
Aluminum 2024 T6	
Titanium (ASTM Grade 3, 99.1% Ti)	
Pure Niobium	Compatible with Exhaust / Useable for uncooled portion of aerospike nozzle

The total aerospike and chamber weight is equal to the combined weight of the structural and cooling jackets. The total aerospike weight also includes the weight of the uncooled nozzle tip. In an attempt to minimize aerospike weight, the inner wall of the aerospike is simplified to a bored hole with a truncated cone at the end, reference Figure 2. This hole also serves to improve aerospike fabrication and allow an open space for running plumbing to the hydrogen cooling jacket.

The total engine weight is equal to the sum of the chamber, aerospike, turbopump, plumbing, and hardware weights, not including propellant weight. System level turbopump weight is a function of the oxidizer-to-fuel ratio and the engine mass flow rate using relationships from Humble *et al.* [11]. In calculating the fuel and oxidizer plumbing weight, a conservative pipe length was assumed to equal twice the total engine length (chamber length plus nozzle length). Ideally the turbopumps will be close to the chamber injector face minimizing the length of the plumbing. A detailed engine layout needs to be accomplished as a future task for increased fidelity in estimating plumbing weight. Hardware weight is assumed equal to a conservative estimate of 5% the sum of the aerospike, chamber, LOX turbopump, LH2 turbopump and plumbing weights. Hardware accounts for rivets, nuts, bolts, wiring, etc. With the known total engine weight, the  $T/W$  is calculated.

## V. Results and Analysis

The enhanced DEAN model was used in two distinct ways. First, trade studies of the solution space and the individual key design variables were performed to understand the influence of the variables on the DEAN design

and to find a new design point meeting the engine performance design goals. Second, the new design point was optimized for maximum thrust-to-weight while meeting reusability and physical constraints.

#### A. Trade Study Design Variables

The key design variables influencing DEAN performance are chamber and aerospike radii at the injector face, chamber length, engine mass flow rate and  $O/F$ . The key design variables influencing DEAN  $T/W$  are engine component material selection and the material strength option (ultimate or yield strength). The model requires other inputs to execute; however, these inputs are secondary design variables for execution of NPSS and TDK. Trade studies were performed on these secondary design variables and, based on the results, a single variable value giving improved NPSS and TDK model flexibility was selected and assigned for the remainder of the work [6]. Turbopump variable inputs remained constant for the trade studies as shown in Table 2.

Key DEAN design variable limits were chosen, as shown in Table 5, constraining the solution space to provide realistic results. For example, the range of chamber length is highly dependent on the range of chamber and aerospike radii at the injector face. Chamber length, chamber radius and aerospike radius have to create a large enough combustion chamber volume equal to or greater than the characteristic length of the propellant to maximize combustion and engine performance. For the trades, the  $O/F$  value was held constant at 6.0; the optimal value found by Simmons [5].

**Table 5 DEAN design variable ranges**

Design Variables	Range
Engine Mass Flow Rate	85 – 130 lb <sub>m</sub> /s (38.6 – 59.0 kg/s)
Chamber Length	14 – 26 in (35.6 – 66 cm)
Chamber Radius at Injector Face	5 – 20 in (12.7 – 50.8 cm)
Aerospike Radius at Injector Face	5 – 20 in (12.7 – 50.8 cm)
Material Strength Option	Ultimate Tensile, Yield
Percent Aerospike Nozzle Truncation	0 – 100%

#### B. Trade & Optimization Studies to find new DEAN design point

To improve engine performance an increase in the engine's expansion ratio is required. This is accomplished by a decrease in throat area or an increase in exit area. Trade studies of the design variables were performed with the goal of finding a new design point meeting the performance design goals with a greater expansion ratio.



Trade studies were initially performed on the engine mass flow rate, chamber length, and aerospike radius at the injector face design variables to understand the influence of each variable of the engine design's performance. The results of the studies showed, without changing the chamber radius, the designer could decrease the engine throat area thus improving the expansion ratio and vacuum performance of the DEAN. Best performance is achieved for an aerospike radius close to the chamber radius at the injector face with a long chamber length and low mass flow rate. However, an engine with these design characteristics may not be physically possible due to high wall temperatures, which may violate the material melting point physical constraint; higher wall temperatures are associated with higher chamber pressures leading to increased performance.

For an aerospike nozzle, the exit area is increased by increasing the chamber exit lip radius, which is a function of the chamber radius at the injector face design variable. A detailed design of experiments (DOE) was performed to evaluate the influence of chamber radii on engine performance. To maximize NPSS convergence, the mass flow rate was held constant at 130 lb<sub>m</sub>/s (59.0 kg/s). The chamber length, aerospike radius, and chamber radius had variable ranges shown in Table 5. Each was varied for a total of 1,784 experiments. Out of the 1,784 experiments, 442 successfully demonstrated potential to meet the overall objectives. Figure 4 plots vacuum specific impulse as a function of chamber radius for the successful design points.

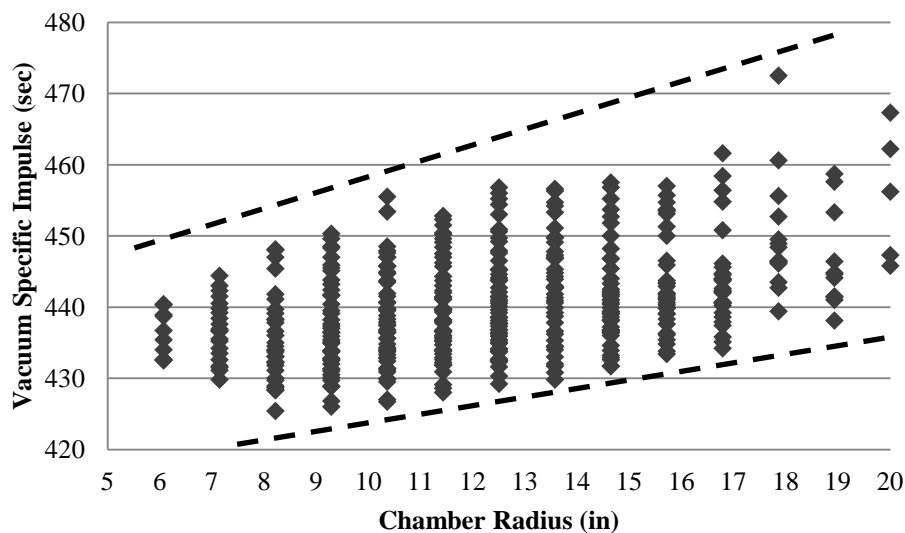


**Figure 4 Influence of chamber radius on vacuum specific impulse**

Figure 4 shows increasing the chamber radius does not automatically equate to a higher vacuum specific impulse. The influence of increasing chamber radius is most clearly recognized at the data points close to the lower dotted line. As chamber radius increases, the expansion ratio increases leading to an increase in vacuum specific

impulse. The data points close to the lower dotted line in Figure 4 represent engine designs with shorter chamber lengths and smaller aerospike radii that result in lower chamber pressures, higher throat areas, lower expansion ratios and lower vacuum specific impulse. In contrast, the data points close to the upper dotted line represent engines with long chamber lengths and aerospike radii close to the chamber radii. The result is higher chamber pressures, smaller throat areas, higher expansion ratios and improved vacuum performance. Clearly seen in Figure 4 is the difference in vacuum specific impulse between the upper and lower ranges is not due to an increase in chamber radius alone.

The influence of chamber radius, aerospike radius and chamber length on vacuum specific impulse can be seen in the results represented in Figure 5 with chamber radius on the x-axis, chamber length on the y-axis and aerospike radius on the z-axis. The shade and size of the boxes in the glyph plot relate to vacuum specific impulse. The small boxes are lower vacuum specific impulse, while the large boxes are higher vacuum specific impulse; the two highest vacuum specific impulse design points are circled for emphasis.

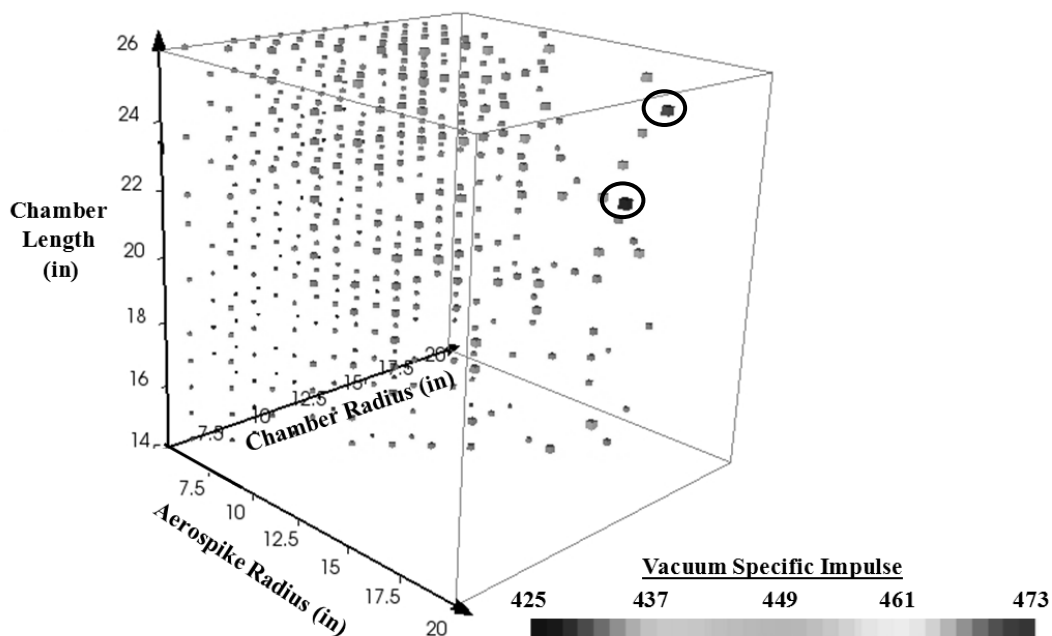


**Figure 5 Influence of design variables on vacuum specific impulse**

The conclusion is to obtain high vacuum specific impulse, increasing chamber radius combined with a long chamber length and an aerospike radius close to the chamber radius is required. The expansion ratio will be larger with increased chamber exit lip radius and a smaller throat area. The high specific impulse designs have high wall

temperatures leading to low  $T/W$  (less desirable). Due to the high wall temperatures, the material strength is lower causing increased structural and cooling jacket thicknesses and engine weight.

Figure 6 highlights the relationship between vacuum specific impulse and  $T/W$ . The vacuum thrust range for the successful designs is 55,000 to 62,000  $\text{lb}_f$  (224.7 to 275.8 kN); higher than the design goal due primarily to the assumed mass flow rate. The vacuum specific impulse design goal of 464 seconds and the  $T/W$  design goal of 106.5 are also shown. The best material selection found in previous work [23] was used to estimate  $T/W$ . The square boxes represent design points where the chamber and/or aerospike maximum wall temperature exceeded the material melting point. The circles represent design points with chamber and/or aerospike maximum wall temperatures above the 60% melting point reusability goal. The diamonds represent design points with wall temperatures below the 60% melting point reusability goal.

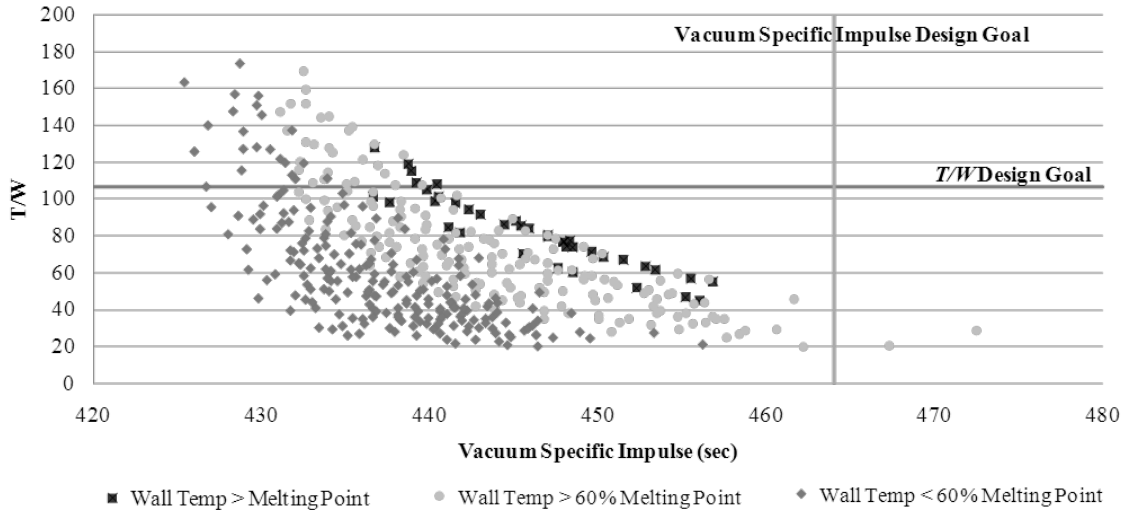


**Figure 6  $T/W$  and vacuum specific impulse of potential DEAN designs**

Surprisingly, acceptable designs both meeting the  $T/W$  design goal and below the wall temperature reusability goal congregate around 425 to 435 seconds vacuum specific impulse. To obtain high vacuum specific impulse, higher wall temperatures are expected with low  $T/W$ . The low  $T/W$  is due to lower material strength from the increased wall and coolant temperatures leading to increased structural jacket thicknesses. Furthermore, higher vacuum specific impulses occur for long chamber lengths and large chamber and aerospike radii leading to more material volume and high component weights.

One result of this study is identifying the need to evaluate the DOE solution space and determine if parameter ranges can be expanded. The acceptable designs led to NPSS numerical convergence with set NPSS inputs (i.e. cooling channel geometry and percentage of oxygen bypassing the turbine); however, potential future designs need

to be explored (i.e. vary mass flow rates). With the current DOE results, the best DEAN designs meeting the thrust and  $T/W$  design goals and meeting physical constraints (both wall temperature and Mach numbers) are the designs with a vacuum specific impulse of 430 seconds. To meet the other design goals (i.e.  $T/W$ ), the vacuum specific impulse design goal cannot currently be met. The result suggests design choices and assumptions need to be readdressed in future efforts to expand the design solution space.

Table 6 identifies an engine that meets the performance design goals but does not meet the  $T/W$  and reusability design goals using the best material selection in [23]. To increase the engine  $T/W$  and lower the performance values closer to the design goals, the aerospike nozzle was truncated. The chamber and aerospike wall percent melting points are extremely high and, realistically, too close to the melting point to be considered practical. Although the engine in Table 6 does meet the vacuum specific impulse performance design goals, the high wall temperatures (chamber and aerospike percent melt) and low  $T/W$  make the design undesirable.

**Table 6 DEAN design meeting performance design goals**

Design Variables		Response Variables	
$O/F$	6.0	Vacuum Thrust	51,225 lb <sub>f</sub> (227.9 kN)
Engine Mass Flow	110 lb <sub>m</sub> /s (50.0 kg/s)	Vacuum Specific Impulse	465.7 s
Chamber Length	21.7 in (55.1 cm)	$T/W$	27.7
Chamber Radius	17.9 in (45.5 cm)	Total Engine Weight	1852.4 lb (840.2 kg)
Aerospike Radius	15.7 in (39.9 cm)	Chamber Percent Melt	93%
Percent Nozzle Truncation	84.50%	Aerospike Percent Melt	92%
		Chamber Pressure	2884 psia (19.9 MPa)
		Throat Area	9.34 in <sup>2</sup> (60.3 cm <sup>2</sup> )

A full-length nozzle DEAN design that does meet the  $T/W$ , reusability and vacuum thrust design goals, but misses the vacuum specific impulse design goal, is tabulated in Table 7. This design was chosen for continued  $T/W$  optimization studies due to meeting the majority of the design goals, including the maximum fluid Mach number physical constraint, as opposed to the design in Table 6.

**Table 7 Best DEAN design variables**

Design Variables		Response Variables	
$O/F$	6.0	Vacuum Thrust	50,161 lb <sub>f</sub> (223.1 kN)
Engine Mass Flow	116.5 lb <sub>m</sub> /s (52.8 kg/s)	Vacuum Specific Impulse	430.6 s
Chamber Length	14.5 in (36.8 cm)	Chamber Pressure	1,548 psia (10.7 MPa)
Chamber Radius	6.0 in (15.2 cm)	Throat Area	18.0 in <sup>2</sup> (116.1 cm <sup>2</sup> )
Aerospike Radius	4.5 in (11.4 cm)	Total Engine Length	26.7 in (67.8 cm)

### C. Engine Thrust-to-Weight Ratio Optimization

With the new design point, the next step focused on optimizing the design for maximum  $T/W$  while meeting the physical structural and reusability constraints. To meet the physical structural constraints, the maximum cooling and structural jacket wall stress must be less than the material's ultimate tensile strength. In order for the DEAN to be considered reusable, the maximum wall temperature compared to the material melting point must be less than or equal to 60%. In addition, for reusability, permanent deformation is unacceptable and the material strength option is set to yield strength with a conservative factor of safety of 1.5.

The component material selection maximizing ("best") and minimizing ("worst")  $T/W$  was found for each engine component to bound potential  $T/W$  values for the new DEAN design. The seven engine components influenced by material selection in the model are chamber cooling and structural jackets, aerospike cooling and structural jackets, aerospike nozzle tip, and hydrogen and oxygen plumbing. The system level hydrogen and oxygen turbopump weight was neglected for this portion of the study since it is a function of engine mass flow rate and not influenced by material selection. Table 8 tabulates the engine component and the corresponding best and worst material selection. The bound  $T/W$  values for the different material strengths are in Table 9. For low density, high strength materials, such as aluminum 7075 T6, the difference in  $T/W$  between ultimate and yield strength is minimal (~3%). However, for highly conductive, high density materials, such as pure copper, there is approximately an 82% decrease in  $T/W$  from changing the material strength option from ultimate tensile to yield strength.

**Table 8 Material selection for maximum and minimum  $T/W$**

Engine Component	Best Material Selection	Worst Material Selection
Chamber Cooling Jacket	Silicon Carbide	Copper
Aerospike Cooling Jacket	Silicon Carbide	Alloy 188
Chamber Structural Jacket	Aluminum 7075 T6	Copper
Aerospike Structural Jacket	Aluminum 7075 T6	Copper
Aerospike Nozzle Tip	Silicon Carbide	Alloy 188
Hydrogen Plumbing	INCOLOY 909	Copper
Oxygen Plumbing	INCONEL 718	Copper

**Table 9 Impact of material strength on  $T/W$**

	Worst Material Selection		Best Material Selection	
	Yield Strength	Ultimate Strength	Yield Strength	Ultimate Strength
$T/W$	12.4	69.2	172.3	176.5

The chamber, and more specifically the chamber structural jacket, accounts for the highest percentage of total engine weight for the worst material selection. Conversely, for the best material selection, the engine component with the highest percentage of total engine weight is the oxidizer turbopump. For different material selections, the engine components with the most influence on total engine weight will be the structural jackets and turbopumps. The influence of the structural jackets is reasonable since the structural jackets have the most volume out of any engine component. As high strength, low density, good conductivity materials are utilized, the combined fuel and oxidizer turbopump weight will remain constant while other components will decrease in weight causing the ratio of turbopump weight to total engine weight to increase. The turbopump influence on overall engine weight is coupled to the  $O/F$  ratio and the engine mass flow rate.

The cooling jacket material selection has very little influence on the engine  $T/W$ ; however, the material selection has a large influence on whether the chamber and aerospike cooling jacket walls will melt. The bar plot in Figure 7 shows the influence of material selection on the maximum wall temperature as a function of material melting point (percent material melting point). NPSS calculates a constant convection heat transfer coefficient on the hot and cold side of the cooling jacket wall. The calculated maximum wall temperature for each material is different only because of differences in the thermal conductivity and strength of the material (required wall thickness). Thicker cooling jackets result in higher maximum wall temperatures (distance between hot gases and coolant). Therefore, the bars representing different materials in Figure 7 correspond to different maximum wall temperatures and cooling jacket thicknesses.

For the current trade study, only one material option for the chamber and three for the aerospike meet the 60% melting point reusability goal. The plumbing and aerospike nozzle tip have very little influence over the engine  $T/W$ . Material selection for those components is kept constant (nickel alloys for the plumbing and silicon carbide for the aerospike nozzle tip).

The best material selection exceeds the  $T/W$  design goal. For the engine components requiring material selection in the DEAN model, the structural jackets have the most influence on the engine  $T/W$ ; therefore, the material selections for only the chamber and aerospike structural jackets were allowed to vary in this trade study. The goal was to find multiple material selections for the structural jackets meeting or exceeding the engine  $T/W$  requirement. Ten material selections meet this requirement for the aerospike and twelve for the chamber structural jackets, 120 total material combinations. The design  $T/W$  range using the material's yield strength to meet reusability constraints

is 14 to 171. Numerous material selections meet or exceed the  $T/W$  design goal of 106.5. Copper chamber structural jackets result in low  $T/W$ . Aluminum 7075 T6 or silicon carbide structural jackets result in high  $T/W$ .

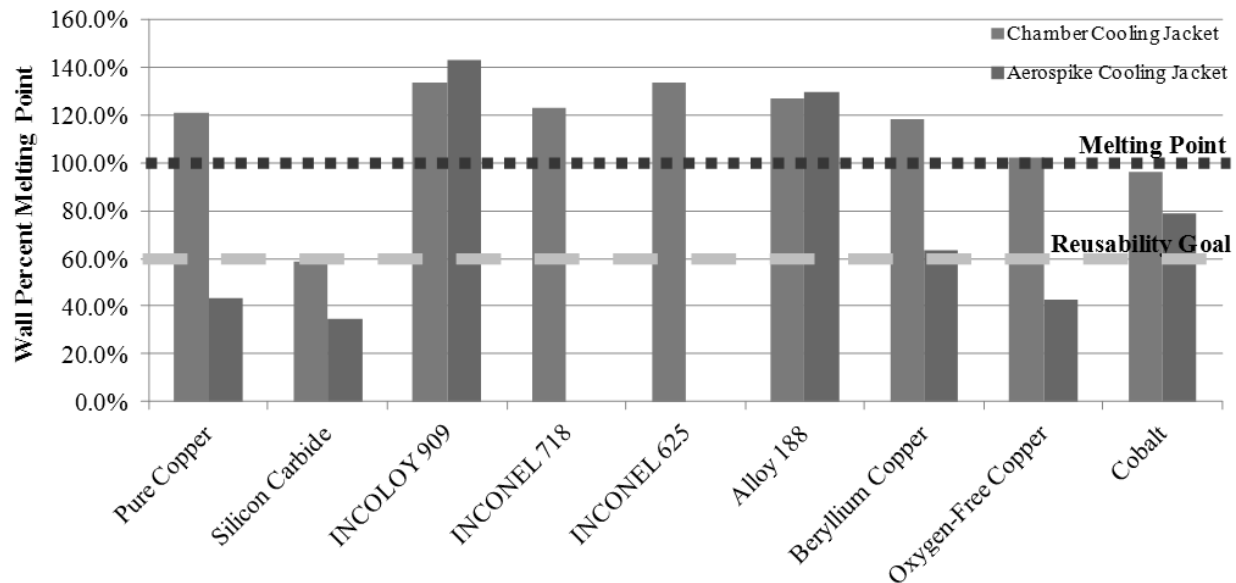


**Figure 7 Influence of material selection on cooling jacket wall temperature**

To improve aerospike manufacturability for a reusable engine, the same material will be utilized for the aerospike cooling jacket, structural jacket and the uncooled aerospike nozzle tip. Although with the highest component  $T/W$ , a silicon carbide aerospike cooling jacket with an aluminum structural jacket would be both difficult to manufacture as well as assemble due to the complex geometry of the nozzle. Using the same material simplifies the process by allowing the manufacturer to fabricate both the structural jacket and cooling jacket at the same time with one piece of material. Therefore, only oxygen-free copper and pure copper remain as potential aerospike materials from Figure 7; the cooling jacket material is the limiting factor for aerospike material selection.

Utilizing oxygen-free copper for all aerospike components had better total engine  $T/W$  over the pure copper. Annealed pure copper and heat-treated oxygen-free copper material properties were incorporated into the system level model. The heat treatment for the oxygen-free copper improves material strength accounting for the difference in the  $T/W$  between the very similar copper materials. To meet the reusability and  $T/W$  design goals, the best manufacturing design used oxygen-free copper for all aerospike components, aluminum and silicon carbide for the chamber and nickel alloys for the plumbing.

Nozzle truncation studies were performed to determine if nozzle truncation leads to improvements in  $T/W$  with minimal performance losses. Results showed  $T/W$  improvements depend on how much the aerospike is

truncated. Initially engine  $T/W$  increases as nozzle truncation increases due to a larger loss in aerospike nozzle mass compared to the performance lost. However, at a certain point a transition occurs where  $T/W$  decreases for increased truncation compared to the full-length nozzle. This transition, occurring at approximately 50% truncation for this study, is due to the loss in performance being greater than the loss in aerospike nozzle mass. For clarity, nozzle truncation refers to a specific length of the nozzle being removed from the full-length nozzle tip. As an example, the vacuum specific impulse,  $T/W$ , and engine length losses at 75% nozzle truncation compared to the full-length nozzle are -3.1%, -1.5%, and -34%, respectively. The benefit of nozzle truncation for upper stage applications is recognized with the engine length. By decreasing the engine length, there are indirect benefits to the total launch vehicle. For example, a shorter upper stage engine leads to a shorter, lighter interstage. Since the current DEAN design does not meet the specific impulse goal, the best DEAN design utilizes the full-length aerospike nozzle for maximum performance neglecting any benefits of nozzle truncation.

#### D. Best DEAN Design

The best DEAN design from this study utilizes the full-length aerospike nozzle using the design variables in Table 10 and materials in Table 11.

**Table 10 Best DEAN design variables**

Design Variables		Response Variables	
$O/F$	6.0	Vacuum Thrust	50,161 lb <sub>f</sub> (223.1 kN)
Engine Mass Flow	116.5 lb <sub>m</sub> /s (52.8 kg/s)	Vacuum Specific Impulse	430.6 s
Chamber Length	14.5 in (36.8 cm)	Thrust-to-Weight Ratio	142.2
Chamber Radius	6.0 in (15.2 cm)	Chamber Pressure	1,548 psia (10.7 MPa)
Aerospike Radius	4.5 in (11.4 cm)	Throat Area	18.0 in <sup>2</sup> (116.1 cm <sup>2</sup> )
		Total Engine Length	26.7 in (67.8 cm)
		Total Engine Weight	352.7 lb (160.0 kg)

**Table 11 Materials for best DEAN design**

Engine Component	Material Selection
Chamber Cooling Jacket	Silicon Carbide
Chamber Structural Jacket	Aluminum 7075 T6
Aerospike Cooling Jacket	Oxygen-Free Copper
Aerospike Structural Jacket	Oxygen-Free Copper
Aerospike Nozzle Tip	Oxygen-Free Copper
Hydrogen Plumbing	INCOLOY 909
Oxygen Plumbing	INCONEL 718



The performance values for the final design meet the vacuum thrust and  $T/W$  design goals; the performance values are 50,161  $\text{lb}_f$  (223.1 kN) vacuum thrust, 430.6 seconds vacuum specific impulse and a  $T/W$  of 142.2. The design also meets the DEAN reusability design goals with a cooling jacket wall percent melting point of 58.6% and 43.0% for the chamber and aerospike, respectively, and with passing the structural analyses using yield strength with a factor of safety of 1.5. The characteristic length,  $L^*$ , for the final design is 37.8 inches (96.0 cm); within the typical range for  $\text{O}_2/\text{H}_2$  engines [8]. The throat area is equal to  $18.0 \text{ in}^2$  ( $116.1 \text{ cm}^2$ ), equating to a radius difference of 0.61 inches (1.6 cm) between the chamber and aerospike throat radii. The engine expansion ratio is equal to 4.37.

Table 12 summarizes the fuel and oxidizer turbopump parameters for the best DEAN design; the input turbopump efficiency values are in Table 2. Five percent of the oxidizer flow bypasses the turbine leading to the lower turbine mass flow rate.

The final engine component mass for the DEAN design is summarized in Table 13. The total thickness of the chamber and aerospike at the injector face is 0.64 and 0.55 inches (1.6 and 1.4 cm), respectively. This thickness is the summation of the cooling jacket wall thickness, cooling channel height, cooling channel cover thickness, and structural jacket thickness. The minimum required structural thickness for the oxidizer and fuel plumbing are 0.02 and 0.03 inches (0.05 and 0.08 cm), respectively.

**Table 12 DEAN turbopump parameters**

	Oxidizer	Fuel
Pump #1 Pressure Ratio	95.9	8.46
Pump #1 Power	-1945.06 HP (-1.45 MW)	-419.28 HP (-0.31 MW)
Pump #2 Pressure Ratio	--	8.46
Pump #2 Power	--	-3163.83 (-2.36 MW)
Pump #1 & #2 Mass Flow Rate	99.86 $\text{lb}_m/\text{s}$ (45.30 $\text{kg/s}$ )	16.64 $\text{lb}_m/\text{s}$ (7.55 $\text{kg/s}$ )
Turbine Pressure Ratio	1.84	1.56
Turbine Power	1945.07 HP (1.45 MW)	3583.11 HP (2.67 MW)
Turbine Mass Flow Rate	94.86 $\text{lb}_m/\text{s}$ (43.03 $\text{kg/s}$ )	16.64 $\text{lb}_m/\text{s}$ (7.55 $\text{kg/s}$ )
Turbopump Shaft Speed (RPM)	32,000	110,000

**Table 13 Engine component mass**

Engine Component	Mass
Chamber	39.1 lb (17.7 kg)
Aerospike	79.4 lb (36.0 kg)
Plumbing	4.3 lb (1.95 kg)
Turbopumps	213.1 lb (96.7 kg)
Hardware	16.8 lb (7.6 kg)
<b>TOTAL ENGINE MASS</b>	<b>352.7 lb (160.0 kg)</b>

The fluid pressure profile through the best DEAN design is shown in Figure 8. The pressure profile shows how the propellant pressures change through the two independent expander cycles until both the oxidizer and fuel have the same pressure in the combustion chamber. Based on the pressures and temperatures at each station, the oxygen becomes supercritical in the cooling jacket and remains supercritical to the injectors. The hydrogen becomes supercritical at the second pump outlet and remains supercritical to the injectors.

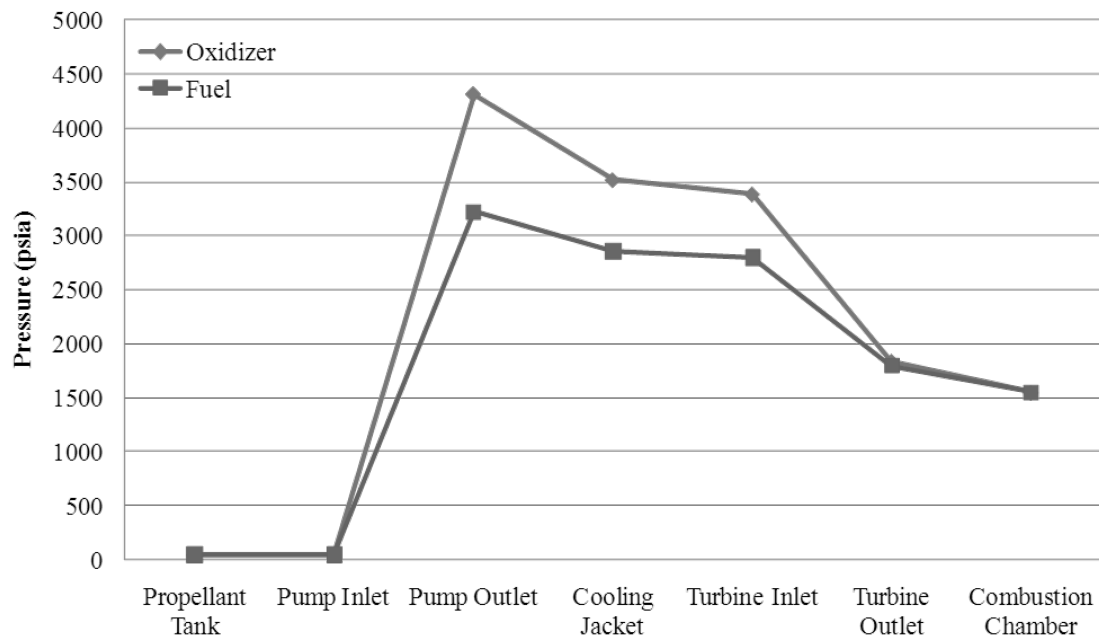
**Figure 8 Best DEAN design fluid pressure profile**

Table 14 tabulates the individual thrust components. The aerospike nozzle exit pressure is equal to 97.7 psia (0.7 MPa) relating to a design altitude of approximately 220 feet (67 m) below sea-level. Due to the small radial geometry of the best DEAN design, the exit pressure is much higher than sea level ambient pressure. The high exit pressure leads to a high  $F_{nondesign}$  value for DEAN operation in vacuum conditions. The total percent boundary layer

loss on the aerospike nozzle is 4.4%, included in the nozzle pressure thrust value. Other performance losses are not included in this study.

**Table 14 Individual thrust components**

Thrust Component	Thrust
Aerospike Nozzle Pressure Thrust	8,216 lb <sub>f</sub> (36.5 kN)
Momentum Thrust	34,314 lb <sub>f</sub> (152.6 kN)
Thrust due to Operation at Altitude other than Design Altitude ( $F_{nondesign}$ )	7,677 lb <sub>f</sub> (34.1 kN)
Chamber Exit Lip Pressure Thrust	-46 lb <sub>f</sub> (-0.2 kN)
Total DEAN Vacuum Thrust	50,161 lb <sub>f</sub> (223.1 kN)

Figure 9 shows the rendered geometry of the best DEAN design. In Figure 9b, due to the chosen aerospike radius design variable, the aerospike portion internal to the chamber is almost linear in nature with a slightly negative slope to the throat. From the orthogonal views, the total thickness of the chamber and aerospike is visible. The total engine length from the injector face to the end of the aerospike tip is 26.7 inches (67.8 cm) with a maximum diameter at the injector face of 12 inches (30.5 cm).

## VI. Application of the DEAN Engine

The DEAN engine was designed with specific goals to perform orbit transfer/upper stage operations. Design trades in performance and  $T/W$  in this study produced a DEAN design missing the vacuum specific impulse goal by 7.3%. This design can still successfully perform orbit transfer/upper stage operations; however, with the lower specific impulse, more propellant may be required to complete the mission compared to the desired engine design meeting all goals. The best method to determine mission impact is to compare with other engines using a full mission analysis (reserved for a future effort).

The DEAN design is a competitor to the Evolved Expendable Launch Vehicle (EELV) upper stage engine, the Delta IV RL10B-2. Compared to the RL10B-2, the DEAN has a 103% improvement in vacuum thrust with a 7.5% decrease in vacuum specific impulse. The DEAN boasts a 281% improvement to the RL10B-2 in engine  $T/W$  utilizing standard metals, alloys, and ceramics. Additionally, the DEAN total engine length and diameter is 69% and 86% less than the stowed RL10B-2 engine. The DEAN does not employ an extendible nozzle like the RL10B-2 thus eliminating moving parts and further improving engine reliability. Although vacuum specific impulse for the DEAN is lower, the main benefits of the DEAN over the RL10B-2 are decreased engine length and weight. With

decreased engine length and weight, the DEAN offers indirect benefits to the entire launch vehicle, such as a shorter and lighter interstage.

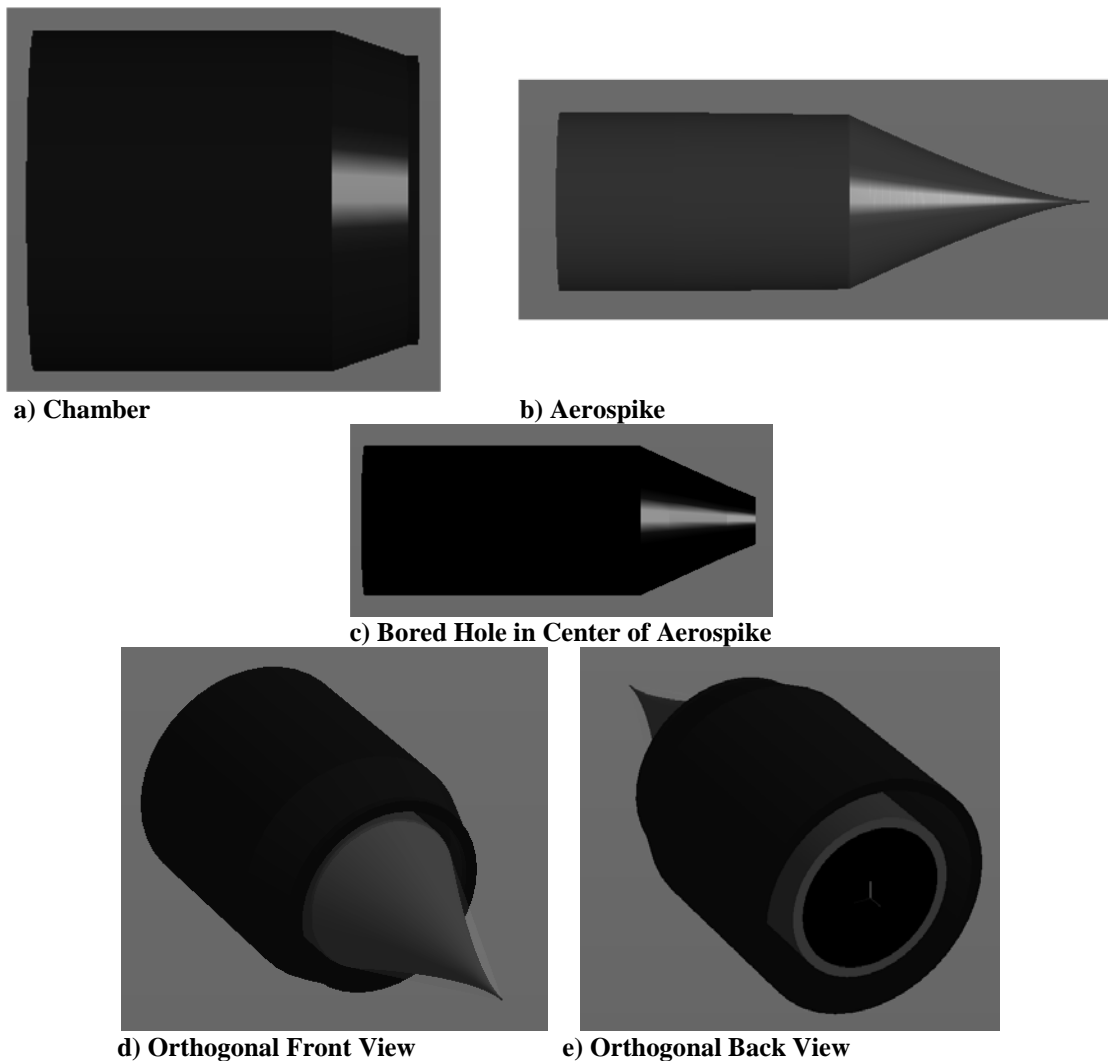


**Figure 9 Best DEAN geometry**

The best DEAN design has applications to other mission areas. For example, the performance from such a small size and low weight engine with reusability characteristics makes this engine useable as a potential air-launch space plane engine. Table 15 summarizes some of the advantages of the current design. With these advantages, the DEAN engine can plausibly serve as the liquid equivalent to the solid motor Pegasus launch vehicle.

**Table 15 Advantages of the DEAN design**

Advantage	Explanation
Compact	The length and diameter of the engine is perfect for applications with packaging restrictions. A small air-launch space plane with the DEAN engine could fit under a B-52 wing and/or fit in the stowage bay of a cargo aircraft.
Lightweight	The low weight adds further fidelity to the DEAN's benefits of being compact.
Ignition Altitude Independent	The aerospike nozzle is operable at any altitude. This enables the DEAN to be used for horizontal launch from conventional aircraft.
Performance Independent of Altitude	The aerospike nozzle can operate at various altitudes with increased performance over conventional bell nozzles.
Testable	The engine could be extensively tested, including hot fire tests of flight units, at sea level facilities without the additional expense of using altitude chamber test facilities.

## VII. Conclusion

Utilizing past AFIT work as a foundation, an enhanced system level DEAN model was created to provide a conservative estimate of engine performance and engine weight without violating physical and reusability constraints. The improvements in modeling demonstrate a need to update previous conclusions about the performance gains of the DEAN. The expansion ratio for aerospike nozzles, and consequently performance, is a function of nozzle geometry and cannot be assumed.

Although the nonlinear calculations in the enhanced system level DEAN model provide added fidelity and accuracy, the linear calculations provide an acceptable approximation for system level studies. The linear calculations drastically improve computation time enabling more rapid exploration of the design space for future design work.

The assumptions in this trade and optimization study conclude this set of engine parameters could not meet all the design goals. A new engine cycle was found meeting the engine thrust-to-weight ratio and reusability design goals while falling short of the vacuum specific impulse design goal. The current design shows potential in applications where engine size and weight are significant constraints. Future direction and efforts to further the DEAN design concept have been identified and warrant further research.

The views expressed in this paper are those of the authors and do not reflect the official policy or position of the U.S. Air Force, the U.S. Department of Defense, or the U.S. Government.

## Acknowledgments

The authors would like to thank the Air Force Research Laboratory for their continued support of this work. Also, thank you to the following for providing the software used in the enhanced DEAN model: the National Aeronautics and Space Administration (NASA) for the Numerical Propulsion System Simulation (NPSS) and Chemical Equilibrium with Applications (CEA) tools, Phoenix Integration for providing ModelCenter, and Software Engineering Associates, Inc for providing Two Dimensional Kinetics (TDK) '04 and information regarding the Angelino approximation method.

## References

- [1] DeGeorge, D. and Fletcher, S. *The Integrated High Payoff Rocket Propulsion Technology Program and Tactical Missile Propulsion Status*. AFRL-PR-EN-TP-2002-214. Pages 1-3.
- [2] Wright, D. *The Upper Stage Engine Technology (USET) Effort*. JANNAF 2004 LPS.
- [3] *Next Generation Engine (NGE) Request for Information*. Solicitation Number: SMC10-55. Department of the Air Force, Air Force Space Command, Space and Missile Systems Center (SMC). September 2010.  
[https://www.fbo.gov/index?s=opportunity&mode=form&id=d23c8a2ed2c27f3ce252c6e702a89a10&tab=core&\\_cview=0](https://www.fbo.gov/index?s=opportunity&mode=form&id=d23c8a2ed2c27f3ce252c6e702a89a10&tab=core&_cview=0).
- [4] Martin, D. *Computational Design of Upperstage Chamber, Aerospike, and Cooling Jacket for Dual-Expander Rocket Engine*. MS thesis, AFIT/GAE/ENY/08-M20. Graduate School of Engineering and Management, Air Force Institute of Technology (AU), Wright-Patterson AFB, OH. March 2008.
- [5] Simmons, J. and Branam, R. *Parametric Study of Dual-Expander Aerospike Nozzle Upper Stage Rocket Engine*. AIAA Journal of Spacecraft and Rockets, Volume 48, Number 2, March – April 2011.
- [6] Hall, J. *Optimized Dual Expander Aerospike Rocket*. MS thesis, AFIT/GAE/ENY/11-M10. Graduate School of Engineering and Management, Air Force Institute of Technology (AU), Wright-Patterson AFB, OH. March 2011.
- [7] Piper, L. *LO<sub>2</sub>/LH<sub>2</sub> Liquid Rocket Engine Cycles*. The Johns Hopkins University, Chemical Propulsion Information Agency operating under contract N00014-91-C-0001. CPTR 92-50, September 1992. Page 5.
- [8] Huzel, D. and Huang, D. *Modern Engineering for Design of Liquid-Propellant Rocket Engines*. Progress in Astronautics and Aeronautics, Volume 147, AIAA, 1992.
- [9] NASA Glenn Research Center. *NPSS User Guide*. Tech Report NPSS v1.6.4, 2006.

- [10] Angelino, G. *Approximate Method for Plug Nozzle Design*. AIAA Journal, Vol. 2, No. 10, October 1964, page 1834 – 1835.
- [11] Humble R., Henry, G., and Larson, W. *Space Propulsion Analysis and Design*. McGraw-Hill, 1995, NY.
- [12] Hagemann, G., Immich, H., Nguyen, T., Dumnov, G. *Advanced Rocket Nozzles*. Journal of Propulsion and Power, Volume 14, Number 5, September – October 1998. Page 627.
- [13] Sutton, G. and Biblarz, O. *Rocket Propulsion Elements*. Seventh Edition. John Wiley & Sons. 2001.
- [14] Incropera, F and DeWitt, D. *Fundamentals of Heat and Mass Transfer*. Fifth Edition. John Wiley & Sons, 2002. Pages 3-11 and 492.
- [15] Buch, A. "Pure Metals Properties: A Scientific-Technical Handbook". ASM International. 1999.
- [16] ASM International. "Engineered Materials Handbook". Desk Edition. 2001. CD-ROM.
- [17] Special Metals. INCOLOY(R) alloy 909. Publication Number SMC-077. Special Metals Corporation, 2004.
- [18] Special Metals. INCONEL(R) alloy 718. Publication Number SMC-045. Special Metals Corporation, 2007.
- [19] Special Metals. INCONEL(R) alloy 625. Publication Number SMC-063. Special Metals Corporation, 2006.
- [20] Haynes International. "Heat-Resistant Alloy at a Glance: Haynes(R) 188 Alloy". Haynes International. 2008.
- [21] Metals Handbook, Vol.2 - Properties and Selection: Nonferrous Alloys and Special-Purpose Materials, ASM International 10th Ed. 1990.
- [22] Ross, Robert B. "Metallic Materials Specification Handbook". 4th Edition. Chapman & Hall. 1992.
- [23] Hall, J., Hartsfield, C., Simmons, J. and Branam, R. *Optimized Dual-Expander Aerospike Nozzle Upper Stage Rocket Engine*. 49th AIAA Aerospace Sciences Meeting and Exhibit. Orlando, FL. 4-7 January 2011.